

EVIDENCE OF POSSIBLE SPIN-ORBIT MISALIGNMENT ALONG THE LINE OF SIGHT IN TRANSITING EXOPLANET SYSTEMS

KEVIN C. SCHLAUFMAN¹

Astronomy and Astrophysics Department, University of California, Santa Cruz, CA 95064

Received 2009 December 24

ABSTRACT

There has lately been intense interest in the degree of alignment between the orbits of transiting exoplanets and the spin of their hosts stars. Indeed, of 26 transiting exoplanet systems with measurements of the Rossiter-McLaughlin (RM) effect, eight have now been found to be significantly spin-orbit misaligned in the plane of the sky. Unfortunately, the RM effect only measures the angle between the orbit of a transiting exoplanet and the spin of its host star projected in the plane of sky, leaving unconstrained the complement misalignment angle between the orbit of the planet and the spin of its host star along the line of sight. I use a simple model of stellar rotation benchmarked with observational data to statistically identify ten exoplanet systems from a sample of 75 for which there is likely a significant degree of misalignment along the line of sight between the orbit of the planet and the spin of its host star. I find that HAT-P-7, HAT-P-14, HAT-P-16, HD 17156, Kepler-5, Kepler-7, TrES-4, WASP-1, WASP-12, and WASP-14 are likely spin-orbit misaligned along the line of sight. All ten systems have host stellar masses M_* in the range $1.2 M_\odot \lesssim M_* \lesssim 1.5 M_\odot$, and the probability of this occurrence by chance is less than one in ten thousand. In addition, the planets in the candidate misaligned systems are preferentially massive and eccentric. I combine the distribution of misalignment in the plane of the sky from RM measurements with the distribution of misalignment along the line of sight from this analysis, and the result suggests that transiting exoplanets are more likely to be aligned along the line of sight than expected given predictions for the spin-orbit misalignment distribution of a population produced entirely by planet-planet scattering or Kozai cycles and tidal friction. For that reason, there are likely two populations of close-in exoplanet systems: a population of aligned systems and a population of apparently misaligned systems in which the processes that lead to misalignment or to the survival of misaligned systems operate more efficiently in systems with massive stars and planets.

Subject headings: planetary systems — planetary systems: formation — stars: rotation — stars: statistics

1. INTRODUCTION

The degree of alignment ψ between the orbit of a transiting exoplanet and the spin of its host star can provide insight into the system's formation. In the Solar System, the angle ψ between the planets' orbits and the spin of the Sun is small, about 7° (e.g. Beck & Giles 2005). That fact provided a key piece of evidence supporting the earliest models of planet formation in the same disk in which the Sun formed. Simple models of close-in exoplanet formation involving assembly near the ice line and quiescent migration through a gaseous protoplanetary disk predict that orbits should have only negligible misalignments with the spin of the host star (e.g. Lin et al. 1996; Ida & Lin 2008a,b). Alternatively, simple models without migration but involving dynamical scattering between newly formed planets and planetesimals at several AU predict that non-negligible misalignments ψ can occur (e.g. Ford et al. 2001; Yu & Tremaine 2001; Papaloizou & Terquem 2001; Terquem & Papaloizou 2002; Marzari & Weidenschilling 2002; Chatterjee et al. 2008; Jurić & Tremaine 2008). In reality, there will be some degree of migration in all massive planetary systems (Ward 1997), and in certain situations migration in multiple systems can still lead to non-

negligible misalignments (Thommes & Lissauer 2003). Moreover, any multiple systems that migrate will likely be dynamically stable before the dissipation of their gaseous parent protoplanetary disk, but dynamically unstable after dissipation (Terquem & Papaloizou 2007; Ogihara & Ida 2009). The Kozai effect (Kozai 1962) and tidal processes might also contribute (e.g. Winn et al. 2005; Fabrycky & Tremaine 2007; Nagasawa et al. 2008; Pont 2009). Despite these complications, the frequency of misaligned systems will provide another constraint on models of planet formation.

I describe the geometry of transiting exoplanet systems according to the conventions of Fabrycky & Winn (2009) in Figure 1. An exoplanet's orbit is defined by the vector \mathbf{n}_p and is inclined relative to the line of sight at an angle i_p that can be measured through transit photometry. Note that the fact that an exoplanet is observed to transit requires that $i_p \approx 90^\circ$. The host star's spin is defined by the vector \mathbf{n}_s and is inclined at an angle i_s relative to the line of sight. The angle λ is the angular distance between the projections of \mathbf{n}_p and \mathbf{n}_s in the plane of the sky, and is observable through the Rossiter-McLaughlin (RM) effect (Rossiter 1924; McLaughlin 1924; Ohta et al. 2005). The RM effect – the detection of an anomalous blueshift and redshift superimposed on the stellar reflex in radial velocity measurements during transit – has lately been used to measure λ for several transiting exoplanet systems (e.g.

kcs@ucolick.org

¹ NSF Graduate Research Fellow

Fabrycky & Winn 2009, and references therein). Indeed, the latest RM measurements described in Triaud et al. (2010, submitted) show that eight of the 26 systems with RM measurements are significantly spin-orbit misaligned in the plane of the sky. Though i_s is not constrained by the RM effect, if all of i_p , i_s , and λ are known, the calculation of the true deprojected angle $\psi \equiv \arccos(\mathbf{n}_p \cdot \mathbf{n}_s)$ between \mathbf{n}_p and \mathbf{n}_s is trivial.

The inclination i_s to the line of sight of stellar spin is difficult to measure for individual stars. If the rotation period of a star is known through photometric observations of starspots moving across its surface, and if the projected rotational velocity $v \sin i$ has been measured, then i_s is easy to compute (e.g. Winn et al. 2007). Astrometry measurements of i_s are also possible in special circumstances (Gizon & Solanki 2003). Unfortunately, period measurements are resource-intensive and require well-sampled and precise photometric time series. They may also be biased toward stars with many starspots and therefore biased toward more active and younger stars. On the other hand, the projection of stellar rotation velocity along the line of sight $v \sin i$ can be measured cheaply by examining the rotational broadening of absorption lines in a single high-resolution stellar spectrum. If the radius of the star is known from other means, it is easy to forward-model the observable quantity $v \sin i$ from the stellar rotation period P_* predicted from theoretical or empirical models given a distribution for i . Monte Carlo simulations can then derive the distribution of possible $v \sin i$ measurements. That distribution can then be compared to observational data for transiting exoplanet systems to determine if the observations are consistent with the alignment of a transiting planet's orbit with the spin of its host star.

Calculating the rotation period of Sun-like stars as a function of mass and time is a tractable problem for stars older than about 650 Myr. First, the rotation period of isolated Sun-like stars monotonically slows down as they age (Kraft 1967). Second, even though a population of Sun-like stars is formed with a broad distribution of periods P_* (Attridge & Herbst 1992; Choi & Herbst 1996), by the time that population is the age of the Hyades and Praesepe (about 650 Myr) the broad distribution has converged to a well-defined function of mass (Tassoul 2000; Irwin & Bouvier 2009). Two classes of physical models have been proposed to explain this early-time behavior: magnetic braking by protostellar disks (e.g. Koenigl 1991; Shu et al. 1994; Collier Cameron et al. 1995) and accretion-driven stellar winds (e.g. Matt & Pudritz 2005). Though the physical process that produces this effect in the first ~ 650 Myr is not yet known, the data (Radick et al. 1987; Prosser et al. 1995; Scholz & Eislöffel 2007) and theoretical models (Keppens et al. 1995; Tassoul 2000) are in agreement on the rotational evolution of Sun-like stars after this time. Indeed, Sun-like stars likely lose angular momentum through magnetized stellar winds (Weber & Davis 1967; Mestel 1968; Kawaler 1988), and their rotation slows as $P_* \propto t^{1/2}$, as described observationally as $v \sin i \propto t^{-1/2}$ by Skumanich (1972).

In this paper, I use a simple empirical model to calculate the rotation period of Sun-like stars as a function of mass and age. I combine that model with a

Monte Carlo simulation to marginalize over the uncertain masses, radii, and ages of a control sample of 866 stars from the Spectroscopic Properties of Cool Stars (SPOCS) catalog of Valenti & Fischer (2005) to determine the expected range of projected rotation $v \sin i$ for each star in the control sample under the assumption that the inclination distribution of the SPOCS sample is isotropic. Likewise, I perform a similar calculation for the host stars of transiting exoplanets, this time assuming alignment between the host star's spin and the orbit of its exoplanet. I identify those transiting exoplanet systems in which the disagreement between the $v \sin i$ predicted from the simple empirical model under the assumption of spin-orbit alignment and the observed $v \sin i$ is larger than the equivalent disagreement for any of the 866 stars in the SPOCS control sample. In particular, those systems that have anomalously small $v \sin i$ measurements relative to the measurement errors and the width of simulated $v \sin i$ distribution are possibly spin-orbit misaligned along the line of sight. I describe the details of my calculation in §2. I discuss my results in the context of close-in planet formation in §3. I summarize my findings in §4.

2. ANALYSIS

I combine the well defined mass-rotation period relation in the Hyades and Praesepe (e.g. Irwin & Bouvier 2009) with the relation $P_* \propto t^{1/2}$ (e.g. Weber & Davis 1967; Mestel 1968; Kawaler 1988) to compute the expected rotation periods of Sun-like stars as a function of mass and age. I use a Monte Carlo simulation to transform that function into a $v \sin i_{sim}$ distribution by marginalizing over the uncertain distributions of stellar mass M_* , radius R_* , age τ_* , and the applicable inclination distribution for the sample. As a result, I can compare the observed $v \sin i_{obs}$ measurements with the mean $v \sin i_{sim}$ estimate from the Monte Carlo simulation to determine the degree of agreement between the two. In order to determine the degree of disagreement that can be attributed to random effects, I compare the measured values of $v \sin i_{obs}$ of Sun-like stars in the Solar Neighborhood from the SPOCS catalog with the mean $v \sin i_{sim}$ from the Monte Carlo simulation given the stellar parameters of those stars and the standard isotropic inclination distribution. In this way, I use the control sample of SPOCS stars to determine a threshold level of disagreement that can be expected between the simple empirical model and observation given the observational uncertainties and the imperfections of the model. I then do a similar calculation for the host stars of transiting exoplanets, this time assuming alignment between the spin of the host star and the orbit of its exoplanet. I identify those exoplanet host stars in which the predicted $v \sin i_{sim}$ disagrees with the observed value $v \sin i_{obs}$ relative to the measurement errors by an amount greater than an equivalent disagreement for any of the 866 stars in the control sample. Systems with $v \sin i_{obs}$ slower than $v \sin i_{sim}$ by an amount large relative to the quoted errors in $v \sin i_{obs}$ and the width of the simulated $v \sin i_{sim}$ distribution given the uncertainty in stellar mass, radius, and age are either systems with rotation properties unlike any star in the control sample or in which the inclination of the transiting planet's orbit i_p and the inclination of

the host star's spin i_s are misaligned. Since the SPOCS sample is representative of the sample of transiting exoplanet host stars, the former is very unlikely. For that reason, the best explanation of the anomalously slow projected rotation is spin-orbit misalignment along the line of sight.

2.1. SPOCS Control Sample

I examine a control sample of stars from the SPOCS catalog of Valenti & Fischer (2005) to quantify the scatter about the simple model. The SPOCS sample selection is described in detail in Marcy et al. (2004). In summary, the bulk of the sample was initially selected from the Hipparcos catalog such that each star has $B - V > 0.55$, is no more than three magnitudes above the main sequence, is not a known spectroscopic binary, and has no stellar companion within two arcseconds. Subsequent spectroscopic measurements of CaII H and K were then used to downselect to those stars with ages $\tau_* \gtrsim 2$ Gyr, though an additional 100 stars with ages between 50 and 500 Myr were later added in. As a result, the SPOCS sample has both young and evolved stars as indicated in Figure 14 of Valenti & Fischer (2005).

In addition, previously unknown spectroscopic binaries were removed from the SPOCS candidate list, so there are no spectroscopic binaries in the final catalog. Short-period low-mass binary companions or exoplanets would have been readily apparent in the original California-Carnegie planet search and would have been announced as such long ago. For those reasons, the rotation properties of stars in SPOCS sample should be unaffected by close companions. Moreover, any overlap between the SPOCS sample and the hosts stars of transiting exoplanets is negligible. Collectively, all of these selections and observations suggest that the SPOCS sample is a fair control sample for this analysis.

2.2. Detailed Description of the Monte Carlo

I model the initial mass-period relation of a 650 Myr population of Sun-like stars by binning the available Hyades and Praesepe data (Radick et al. 1987; Prosser et al. 1995; Scholz & Eislöffel 2007) as summarized in Irwin & Bouvier (2009) in $0.1 M_\odot$ bins. The Irwin & Bouvier (2009) data only extends up to about $1.2 M_\odot$, so I supplement it with average rotation periods for more massive field stars as presented in McNally (1965). I use natural cubic splines to interpolate the binned and supplemented data and find that it minimizes the sum of square residuals relative to high-order polynomial interpolation. I determine the expected rotation period of a Sun-like star as a function of mass and age by evolving the initial condition set by the stellar mass according to the relation (e.g. Weber & Davis 1967; Mestel 1968; Kawaler 1988)

$$P_*(M_*, \tau_*) = P_{*,0}(M_*) \left(\frac{\tau_*}{650 \text{ Myr}} \right)^{1/2} \quad (1)$$

where $P_{*,0}(M_*)$ can be approximated as a fifth-order polynomial in M_* with coefficients in increasing order (5.558509, -77.843724, 357.387761, -502.288156, 282.908686, -56.329952). I summarize my technique in Figure 2.

The model described above is likely too simplistic, the relevant input parameters (stellar mass, radius, and age) are all uncertain, and the output (stellar period) is difficult to observe. For those reasons, I use a Monte Carlo simulation to determine the range of observable $v \sin i_{sim}$ expected for a sample of stars given mass, radius, and age as well as the uncertainties in each of those quantities plus the appropriate inclination distribution for that sample. In order to determine the degree of disagreement between the $\overline{v \sin i_{sim}}$ predicted from the simple empirical model and the observed $v \sin i_{obs}$ that can be expected given the observational uncertainties and the imperfections of the simple empirical model, I use the control sample of stars from the SPOCS catalog.

For each star in the SPOCS catalog, I use the estimated stellar mass and uncertainty M_* and σ_M (column 9 of Table 9), estimated stellar radius and uncertainty R_* and σ_R (column 8 of Table 9), and age range $\Delta\tau$ (column 14 of Table 9). In the Monte Carlo, I sample each star's mass from a uniform distribution in mass between $M_* - \sigma_M/2$ and $M_* + \sigma_M/2$, its radius from a uniform distribution in radius between $R_* - \sigma_R/2$ and $R_* + \sigma_R/2$, and its age from a uniform distribution in age between the given lower and upper age limits. I sample the inclination to the line of sight of each star's rotation axis from the standard random distribution $i \sim \arccos(1-U)$, where U is drawn uniformly from the interval $[0,1]$. Using these parameters, I evolve the initial period given by the randomly selected mass and the initial period-mass relation described in Figure 2 to the randomly selected age of the system according to Equation 1. I then compute $v \sin i_{sim}$ using the randomly generated radius of the star and its randomly selected inclination. I repeat this process 1000 times and thereby derive for each star the distribution of possible $v \sin i_{sim}$ values, its mean $\overline{v \sin i_{sim}}$, as well as the width of the distribution σ_{sim} . I compare the predicted $\overline{v \sin i_{sim}}$ with the observed $v \sin i_{obs}$ relative to the width of the Monte Carlo distribution σ_{sim} and the error in the observed $v \sin i_{obs}$ measurement σ_{obs} through the rotation statistic Θ :

$$\Theta \equiv \frac{\overline{v \sin i_{sim}} - v \sin i_{obs}}{\sqrt{\sigma_{obs}^2 + \sigma_{sim}^2}} \quad (2)$$

Note that large positive (negative) values of Θ indicate slower (faster) than expected $v \sin i$ values. Stars that are well fit by the model will have small absolute values of Θ .

I repeat this calculation on each of the 866 stars from the SPOCS catalog with $M_* < 1.5 M_\odot$, assuming the standard isotropic distribution of inclination. This distribution of Θ is the null hypothesis that I will use to compare to the distribution of Θ measured in the transiting exoplanet systems under the assumption of spin-orbit alignment.

I collected the properties of the 80 transiting exoplanets systems known as of May 2010, of which the 75 listed in Table 1 have measured mass, radius, $v \sin i_{obs}$, and orbital inclination. In this case, the stellar masses and radii are more precisely measured than those available in the SPOCS catalog, and the inclination of each exoplanet's orbit is known from transit photometry. I again use a Monte Carlo simulation to determine the range of

observable $v \sin i_{sim}$. I use the measured values for each star’s mass and radius, and I sample each star’s age uniformly between lower and upper bounds for its age from the literature. If there are no age estimates available in the literature, I sample the age of the star uniformly between 650 Myr (the age of the Hyades and Praesepe) and its main sequence lifetime. If there are only upper limits on $v \sin i_{obs}$ in the literature, I assume that the true value corresponds to the published upper-limit, as this is the most conservative way to approach a search for stars with anomalously slow projected rotation. In those situations, I assume that the error in $v \sin i_{obs}$ is 1 km s^{-1} . I assume that the inclination of the host star’s spin relative to the line of sight i_s is the same the inclination of the exoplanet’s orbit i_p . I repeat this process 1000 times and compute the rotation statistic Θ for each stellar host; I report the results of this calculation in Table 1.

2.3. Results

I plot the distribution of Θ for both samples in Figure 3. The Θ distribution of the control sample peaks near $\Theta = 0$, indicating that the simple empirical model is accurate in that the expected residual between the model and the observations is close to zero. The distribution of Θ falls off quickly as Θ increases, and there are no control stars from the SPOCS catalog with $\Theta > 2.9$. However, there does exist a tail of stars with much larger than expected $v \sin i$ values, and therefore large negative Θ values. In other words, some stars in the control sample of SPOCS stars are fast rotators; this is to be expected in any sample of Sun-like field stars. On the other hand, there is no tail of SPOCS stars rotating arbitrarily more slowly than the simple empirical model predicts. For that reason, host stars of exoplanets that are observed to have $\Theta > 2.9$ are apparently unlike any of the 866 stars in the control sample – either they rotate more slowly relative to the model than any star in the control sample or their anomalously slow projected rotation is due to a pole-on view of the star and therefore spin-orbit misalignment.

I define fast rotators as those stars with $\Theta < -5.2$, corresponding to the fastest 5% of the Θ distribution for the SPOCS control sample. Note that the fraction of fast rotators in each sample is statistically indistinguishable – about $5\% \pm 3\%$ in the SPOCS sample and about $7\% \pm 3\%$ in the transiting exoplanet host star sample. The consistency of the two samples in the fraction of stars that are fast rotators is in sharp contrast to the disparity at the other end of the distribution. Also, the peak of the Θ distribution of transiting exoplanet systems is offset to more negative values of Θ (and therefore faster rotation) than the field star sample. Nevertheless, the distribution of the sample mean of Θ for the 90% of the SPOCS control sample with $-5.2 < \Theta < 2$ is $\bar{\Theta} = -0.25 \pm 0.19$; for the host stars of transiting exoplanets an equivalent calculation yields $\bar{\Theta} = -0.49 \pm 0.19$. I plot Θ as a function of stellar mass for both samples in Figure 4. There is a very sharp cutoff in the control sample at $\Theta \approx 2$ at all masses, and this sharp cutoff is due to lack of a constraint on the inclination of individual stars in the control sample. As a result, σ_{sim}^2 in Equation 2 can be large, resulting in small values of Θ .

I find that HAT-P-7, HAT-P-14, HAT-P-16, HD 17156, Kepler-5, Kepler-7, TrES-4, WASP-1, WASP-12, and

WASP-14 have $\Theta > 2.9$, indicating $v \sin i_{obs}$ too small to be explained by the uncertainties in their masses, radii, or ages if each star’s spin and its exoplanet’s orbit have the same inclination to the line of sight. Unless the host stars of these transiting exoplanets are slower rotators relative to the model prediction than any of the 866 stars in the control sample from the SPOCS catalog, the most natural explanation for these discrepancies is that the inclination of the spin of these host stars i_s is significantly different than the inclination of their exoplanet’s orbit i_p . If these anomalously slow projected rotation values are the result of spin-orbit misalignment, then the difference between $v \sin i_{obs}$ and $v \sin i_{sim}$ can be used to compute the four possible degenerate values of i_s (because $\sin i$ is not one-to-one for $0^\circ \leq i < 360^\circ$). I report these values for the potentially spin-orbit misaligned systems in Table 2. I also identify CoRoT-2, HAT-P-2, HD 189733, Kepler-8, and XO-3 as fast rotators. Note that CoRoT-2 (Alonso et al. 2008) and HD 189733 (Bouchy et al. 2005) are known to be more active than the Sun, and therefore potential fast rotators. HAT-P-2 has been observed to have a large radial velocity jitter, which may indicate an active and possibly quickly rotating star (Bakos et al. 2007a).

All ten candidate misaligned systems have host stellar mass $M_* \gtrsim 1.2 M_\odot$. Again, either these stars have rotation properties unlike any of the 276 control stars in the mass range $1.2 M_\odot \leq M_* \leq 1.5 M_\odot$, or these stars are observed pole-on and therefore spin-orbit misaligned.

2.4. Verification of the Robustness of This Result

In order to verify the robustness of this result, I have repeated my calculations with several different sets of input parameters. Indeed, there are two potentially uncertain inputs to my simple empirical model: the power-law exponent α in the relation $P_* \propto t^\alpha$ and the ages of the stars in the SPOCS control sample. It is certain that the rotation of isolated Sun-like stars slows down with time, so $\alpha > 0$ always. To determine if my result is sensitive to α , I have repeated my calculation for $\alpha = 1/3$, $\alpha = 2/3$, and $\alpha = 1$. If $\alpha = 1/3$, then all of the systems identified with anomalously slow projected rotation in §2.3 are again identified as anomalously slow projected rotators. If $\alpha = 2/3$, eight of the original ten systems are identified as anomalously slow projected rotators (HAT-P-7, HAT-P-14, Kepler-5, Kepler-7, HD 17156, TrES-4, WASP-12, and WASP-14). If $\alpha = 1$, only three of the original ten systems are identified as anomalously slow projected rotators (HAT-P-7, HAT-P-14, and WASP-14).

I have also redone my calculation using a completely uninformative prior on the ages of the stars in SPOCS sample. That is, I assumed that the age of each star was uniformly distributed between 650 Myr and its main sequence lifetime. Again, all ten systems identified in §2.3 as anomalously slow projected rotators and therefore possibly spin-orbit misaligned are again identified in this case.

Angular momentum exchange between a host star and its close-in planetary companion is also unlikely to significantly slow the rotation of the host star and produce an anomalously slow projected rotation velocity. For that to occur, the transfer of angular momentum from host star to exoplanet via tidal forces requires the rotation period of the star to be shorter than the orbital period of the

planet. Indeed, the median orbital period of the transiting planets orbiting the stars identified as anomalously slow projected rotators is $P \approx 3.2$ days, while the median expected rotation period of their host stars is $P_* \approx 6.3$ days.

The presence of slightly evolved stars among the host stars of transiting exoplanets will also not produce false identifications as anomalously slow projected rotators. To see why, note that there are also slightly evolved stars in the control sample of SPOCS stars and recall that the threshold Θ required to identify a star as an anomalously slow projected rotator was set by the maximum disagreement between model and observation in the control sample. In other words, the presence of slightly evolved stars has already been accounted for in setting the threshold. I plot in Figure 5 the distribution of the SPOCS sample in a theoretical HR diagram along with those transiting exoplanet hosts with trigonometric parallaxes. I also indicate the locations of those stellar hosts that I identified as anomalously slow projected rotators and therefore potentially spin-orbit misaligned systems. Figure 5 shows that many of the systems I identified as anomalously slow projected rotators appear to be evolving off of the zero-age main sequence (ZAMS). Nevertheless, the fact that there are many stars in the control sample of SPOCS stars in similar evolutionary states suggests that the effects of stellar evolution on the rotation properties of evolved stars have already been accounted for in my analysis. Moreover, there are several hosts of transiting exoplanets that have evolved off of the ZAMS that I do not identify as anomalously slow projected rotators. Collectively, these facts suggest that effects of stellar evolution cannot explain the rotation properties of the ten systems I identified as anomalously slow projected rotators.

Additional selection effects in either the SPOCS control sample or the transiting exoplanet sample are unlikely to affect this result. Indeed, the fact that SPOCS stars were preferentially selected to be those stars with small enough $v \sin i$ to enable high precision Doppler radial velocity measurements biases my control sample to smaller $v \sin i$ at fixed stellar mass and age. However, since the candidate spin-orbit misaligned stars appear to have anomalously slow projected rotation, the bias acts against the false identification of a star as an anomalously slow projected rotator. Though magnitude-limited transit surveys are biased toward stars slightly more massive than the Sun, there are 276 stars in the control sample with $M_* \geq 1.2 M_\odot$ to compare with. In addition, though targeted transit surveys are biased toward less active stars, the control sample of SPOCS stars is similarly biased. Transit surveys should also not be biased toward evolved stars, as though both transit probability and transit duration increase linearly with host stellar radius (favoring evolved systems), transit depth decreases quadratically with host stellar radius (favoring unevolved systems). For that reason, the chance of detecting a transiting planet is roughly insensitive to host stellar radius.

2.5. Comparison with Rossiter-McLaughlin Measurements

For the anomalously slow projected rotators identified in §2.3, I list in Table 2 the inclination to the line of sight of the stellar rotation axis if the anomalous pro-

jected rotation is due to spin-orbit misalignment along the line of sight. I also note published RM measurements for four of the systems I identify as apparent slow projected rotators; HAT-P-7 and WASP-14 has been identified as a spin-orbit misaligned system (Winn et al. 2009b; Johnson et al. 2009), while HD 17156 and TrES-4 are consistent with spin-orbit alignment in the plane of the sky (Narita et al. 2009, 2010).

Though HD 17156 is consistent with spin-orbit alignment in the plane of the sky from RM measurements, my technique measures misalignment along the line of sight. There is other circumstantial evidence that HD 17156 is misaligned along the line of sight. Fischer et al. (2007) measured a $v \sin i = 2.6 \text{ km s}^{-1}$, a stellar radius $R_* = 1.47 R_\odot$ and used Ca II H and K to infer a rotation period $P_* = 12.8$ days. If the system has $i = 90^\circ$, then a period $P_* = 12.8$ days and the inferred stellar radius $R_* = 1.47 R_\odot$ implies $v \sin i = 5.8 \text{ km s}^{-1}$ (as compared to $v \sin i = 6.9 \text{ km s}^{-1}$ expected based on my simple model). Clearly, it's possible that in this case the activity indicator gives a spurious period estimate; still, if the discrepancy is due to misalignment then $i_s = 26^\circ$ (as compared to $i_s = 22^\circ$ degrees from my measurement).

TrES-4 is consistent with alignment in the plane of the sky from measurements of the RM effect. However, that is a different angle than that measured through my analysis. It could be that the geometry of the TrES-4 system is apparently aligned in the plane of the sky but misaligned along the line of sight; alternatively, TrES-4 could simply be an anomalously slow rotator.

I find that ten of the 75 systems in Table 1 have anomalously slow projected rotation and are likely spin-orbit misaligned along the line of sight. In contrast, the latest Rossiter-McLaughlin measurements reported and summarized in Triana et al. (2010, submitted) suggest that eight of the 26 systems with RM measurements have significant spin-orbit misalignment in the plane of the sky. The higher fraction of systems observed to be misaligned by the RM effect is expected, as the RM effect can detect much smaller degrees of misalignment than the coarser technique described here. Assume for the moment that the smallest degree of misalignment this technique can identify is $|i_p - i_s|_{\min} \approx 50^\circ$ (as suggested by the minimum difference from Table 2). Of the 26 systems with measurements of the RM effect, six have $|\lambda| \gtrsim 50^\circ$. At the same time, the slightly higher incidence of misaligned systems in the sample of RM measurements might be related to the fact that RM measurements are resource intensive. That is, systems that seem to have a higher a priori probability of spin-orbit misalignment based on the current understanding of spin-orbit misalignment (e.g. eccentric systems) are more likely to be targeted for RM measurement. The fact that this analysis includes all known transiting exoplanet systems without the targeting biases inherent in the current sample of RM measurements may even produce a less biased spin-orbit misalignment distribution.

3. DISCUSSION

I identify ten host stars of transiting exoplanet systems in which either the host star is more slowly rotating relative to the simple model than any of the stars in the control sample of SPOCS stars or in which the star is viewed pole-on and the system is spin-orbit misaligned.

This degeneracy can be broken for at least Kepler-5 and Kepler-7, as high precision Kepler photometry should reveal their rotation periods. If the periods are indeed short, then the small observed $v \sin i$ indicates spin-orbit misalignment along the line of sight. Alternatively, if the observed rotation periods are long, then Kepler-5 and Kepler-7 are systems in which the host star has somehow lost angular momentum much more quickly than expected by models of Sun-like stellar spin-down. High precision photometry from other sources might enable similar measurements for the other systems identified as anomalously slow projected rotators.

All ten of the candidate misaligned systems have host stars more massive than the Sun. To determine the significance of this observation, I performed a Monte Carlo simulation in which I randomly selected with replacement ten stars from the 75 listed in Table 1. I repeated this process 10^6 times. Less than 0.01% of the Monte Carlo trials produced a sample in which all ten stars had $1.2 M_\odot \lesssim M_* \lesssim 1.5 M_\odot$. Therefore, the probability that all ten candidate misaligned systems would be identified around massive stars by chance is less than one in ten thousand. Similarly, the median mass of the planets in the candidate misaligned systems is 2 ± 0.6 Jupiter-masses, while the median mass of the whole sample of 75 systems is 1 ± 0.1 Jupiter-masses. Interestingly, there may be a hint of the same apparent overrepresentation of massive planets in spin-orbit misaligned systems from Rossiter-McLaughlin measurements (Torres et al. 2010).

Eccentricity also seems to be related to misalignment probability. Indeed, of the nine transiting systems with FGK stellar hosts and eccentricity $e > 0.1$ (HD 80606, HD 17156, HAT-P-2, WASP-8, XO-3, HAT-P-11, WASP-17, CoRoT-9, and HAT-P-14), there is now evidence from either measurements of the RM effect or this analysis that six of those systems are significantly misaligned (HD 80606, HD 17156, WASP-8, XO-3, WASP-17, and HAT-P-14). The other three systems are unlikely to be observed to be spin-orbit misaligned for a number of reasons: HAT-P-2 is likely an intrinsically fast-rotator and therefore unlikely to be identified as misaligned along the line of sight by the method described in this paper even if it does have significant spin-orbit misalignment along the line of sight, HAT-P-11 may have too small a radius for measurements of the RM effect, and CoRoT-9 has the largest pericenter distance by far of the known transiting planets and almost certainly has had a different evolutionary history than the other known transiting planets. To determine the significance of the apparent correlation between eccentricity and spin-orbit misalignment, I performed a Monte Carlo simulation to determine the expected number of systems with eccentricity $e > 0.1$ from a sample of 16 transiting systems – the total number of significantly misaligned systems from RM measurements and this analysis – expected if spin-orbit misalignment is unrelated to eccentricity. I randomly selected with replacement the eccentricities of 16 planets from the 75 systems listed in Table 1, and I repeated this process 10^6 times. I find that the mean number of systems with $e > 0.1$ in a sample of 16 systems under the assumption that eccentricity is unrelated to spin-orbit misalignment is 2 ± 2 . The observation of six systems with $e > 0.1$ from a random sample of 16 systems occurs in less than one in 150 trials, indicating that eccentricity

and spin-orbit misalignment are related.

In an attempt to derive some constraint on the underlying spin-orbit misalignment distribution in the 75 systems in Table 1, I performed two completeness calculations for two different i_s distributions resulting from two different ψ distributions: (1) corresponding to planet-planet scattering (e.g. Chatterjee et al. 2008), a case in which the inclination of the host star is completely independent of the alignment of the orbit of its planet $i_s \sim \arccos(1 - U)$, where $U \sim \text{Unif}(0,1)$; and (2) corresponding to Kozai cycles and tidal friction (e.g. Fabrycky & Tremaine 2007), a case in which the distribution of i_s is derived from the ψ distribution as given in Figure 10 of Fabrycky & Tremaine (2007) and the λ distribution as given in the RM compilation in Table 5 of Triana et al. (2010, submitted). Assuming a threshold detectable misalignment that corresponds to the smallest degree of misalignment identified ($|i_p - i_s| \gtrsim 50^\circ$) in 75 systems, I find that the expected number of detections in case (1) is 17 ± 4 and in case (2) it is 27 ± 4 . Even though each individual system in this analysis is securely identified as an anomalously slow projected rotator and therefore possibly spin-orbit misaligned, both completeness calculations are strongly dependent on the smallest degree of misalignment this technique can identify. That quantity is uncertain, and as such more data is necessary before any conclusive statements about distribution of spin-orbit alignments is made. The full sample of Kepler transiting planet detections and host star properties available at the end of its four year mission might resolve this issue.

Collectively, this analysis indicates that predictions of spin-orbit misalignment for a population of close-in planets entirely produced by planet-planet scattering or Kozai cycles with tidal friction overpredict the number of misaligned systems. As a result, there seems to be two populations of close-in planets: a population that is spin-orbit aligned and a population that is apparently spin-orbit misaligned. The processes that lead to misalignment or to the survival of misaligned systems seem to operate most efficiently in systems with massive host stars and planets. Indeed, the striking appearance of candidate misaligned systems at $M_* \gtrsim 1.2 M_\odot$ in Figure 4 indicates that the processes that lead to spin-orbit misalignment and survival are threshold processes, similar to the rapid increase in exoplanet incidence with host stellar metallicity (e.g. Santos et al. 2004; Fischer & Valenti 2005). In this case, the transition to frequent apparent spin-orbit misalignment occurs at the same stellar mass at which Sun-like stars with near solar metallicity develop radiative envelopes. This dramatic change in stellar structure will likely strongly effect the poorly-understood tidal processes that play a major role in the formation, evolution, and long-term survival of spin-orbit misaligned systems.

4. CONCLUSION

There are ten transiting exoplanet systems from a larger sample of 75 systems in which the projected rotation velocity of the host star assuming spin-orbit alignment is apparently smaller relative to a simple empirical model of stellar spin-down than any of 866 stars in a representative control sample of stars in the same mass range from the Spectroscopic Properties of Cool Stars

(SPOCS) catalog: HAT-P-7, HAT-P-14, HAT-P-16, HD 17156, Kepler-5, Kepler-7, TrES-4, WASP-1, WASP-12, and WASP-14. Unless the host stars of these transiting exoplanets are slower rotators relative to the model prediction than any of the 866 stars in the representative control sample, the anomalously low $v \sin i$ values are best explained by a pole-on view of the star and therefore spin-orbit misalignment. I only identify significant possible spin-orbit misalignment in systems with host stars more massive than the Sun, as in all ten systems the host stars have stellar masses M_* in the range $1.2 M_\odot \lesssim M_* \lesssim 1.5 M_\odot$. This observation is significant, as there is less than a one in ten thousand chance of its occurrence by chance. There is evidence that systems with massive and eccentric planets are also those most likely to be significantly spin-orbit misaligned. Given current measurements of the Rossiter-McLaughlin effect and frequency of misalignment along the line of sight determined in this analysis, models of close-in planet formation invoking planet-planet scattering or Kozai cycles and tidal friction alone overpredict the number of misaligned systems. As a result, there seems to be two populations of close-in planets: those that are aligned and those that are apparently misaligned. The process that leads to misalignment or survival of misaligned systems likely operates more efficiently in systems with both massive stars and planets. Interestingly, apparently misaligned systems appear to occur preferentially in systems in which the envelope of the host star is radiative, and this transition in stellar structure is likely related through tidal processes to the formation, evolution, and long-term survival of spin-orbit misaligned systems.

I thank Greg Laughlin and Connie Rockosi for useful comments and conversation. This research has made use of NASA's Astrophysics Data System Bibliographic Services. This material is based upon work supported under a National Science Foundation Graduate Research Fellowship.

REFERENCES

- Aigrain, S., et al. 2008, *A&A*, 488, L43
 Alonso, R., et al. 2008, *A&A*, 482, L21
 Anderson, D. R., et al. 2010, *ApJ*, 709, 159
 Attridge, J. M., & Herbst, W. 1992, *ApJ*, 398, L61
 Bakos, G. Á., et al. 2007, *ApJ*, 670, 826
 Bakos, G. Á., et al. 2007, *ApJ*, 671, L173
 Bakos, G. Á., et al. 2009, *ApJ*, 696, 1950
 Bakos, G. Á., et al. 2009, *ApJ*, 707, 446
 Bakos, G. Á., et al. 2010, *ApJ*, 710, 1724
 Barge, P., et al. 2008, *A&A*, 482, L17
 Bean, J. L., et al. 2008, *A&A*, 486, 1039
 Beck, J. G., & Giles, P. 2005, *ApJ*, 621, L153
 Borucki, W. J., et al. 2010, *ApJ*, 713, L126
 Bouchy, F., et al. 2005, *A&A*, 444, L15
 Bouchy, F., et al. 2008, *A&A*, 482, L25
 Buchhave, L. A., et al. 2010, *arXiv:1005.2009*
 Burke, C. J., et al. 2007, *ApJ*, 671, 2115
 Burke, C. J., et al. 2008, *ApJ*, 686, 1331
 Cameron, A. C., et al. 2007, *MNRAS*, 375, 951
 Charbonneau, D., et al. 2009, *Nature*, 462, 891
 Chatterjee, S., Ford, E. B., Matsumura, S., & Rasio, F. A. 2008, *ApJ*, 686, 580
 Choi, P. I., & Herbst, W. 1996, *AJ*, 111, 283
 Christian, D. J., et al. 2009, *MNRAS*, 392, 1585
 Collier Cameron, A., Campbell, C. G., & Quaintrell, H. 1995, *A&A*, 298, 133
 Daemgen, S., Hormuth, F., Brandner, W., Bergfors, C., Janson, M., Hippler, S., & Henning, T. 2009, *A&A*, 498, 567
 Deeg, H. J., et al. 2010, *Nature*, 464, 384
 Deleuil, M., et al. 2008, *A&A*, 491, 889
 Dunham, E. W., et al. 2010, *ApJ*, 713, L136
 Fabrycky, D., & Tremaine, S. 2007, *ApJ*, 669, 1298
 Fabrycky, D. C., & Winn, J. N. 2009, *ApJ*, 696, 1230
 Fernandez, J. M., Holman, M. J., Winn, J. N., Torres, G., Shporer, A., Mazeh, T., Esquerdo, G. A., & Everett, M. E. 2009, *AJ*, 137, 4911
 Fischer, D. A., & Valenti, J. 2005, *ApJ*, 622, 1102
 Fischer, D. A., et al. 2007, *ApJ*, 669, 1336
 Ford, E. B., Havlickova, M., & Rasio, F. A. 2001, *Icarus*, 150, 303
 Fossey, S. J., Waldmann, I. P., & Kipping, D. M. 2009, *MNRAS*, 396, L16
 Fridlund, M., et al. 2010, *A&A*, 512, A14
 Gibson, N. P., et al. 2008, *A&A*, 492, 603
 Gillon, M., Pont, F., Moutou, C., Bouchy, F., Courbin, F., Sohy, S., & Magain, P. 2006, *A&A*, 459, 249
 Gillon, M., et al. 2009, *A&A*, 496, 259
 Gillon, M., et al. 2009, *A&A*, 501, 785
 Gizon, L., & Solanki, S. K. 2003, *ApJ*, 589, 1009
 Hartman, J. D., et al. 2009, *ApJ*, 706, 785
 Hebb, L., et al. 2009, *ApJ*, 693, 1920
 Hebb, L., et al. 2010, *ApJ*, 708, 224
 Hellier, C., et al. 2009, *ApJ*, 690, L89
 Hellier, C., et al. 2009, *Nature*, 460, 1098
 Ida, S., & Lin, D. N. C. 2008, *ApJ*, 673, 487
 Ida, S., & Lin, D. N. C. 2008, *ApJ*, 685, 584
 Irwin, J., & Bouvier, J. 2009, *IAU Symposium*, 258, 363
 Jenkins, J. M., et al. 2010, *arXiv:1001.0416*
 Johns-Krull, C. M., et al. 2008, *ApJ*, 677, 657
 Johnson, J. A., et al. 2008, *ApJ*, 686, 649
 Johnson, J. A., Winn, J. N., Albrecht, S., Howard, A. W., Marcy, G. W., & Gazak, J. Z. 2009, *PASP*, 121, 1104
 Joshi, Y. C., et al. 2009, *MNRAS*, 392, 1532
 Jurić, M., & Tremaine, S. 2008, *ApJ*, 686, 603
 Kawaler, S. D. 1988, *ApJ*, 333, 236
 Keppens, R., MacGregor, K. B., & Charbonneau, P. 1995, *A&A*, 294, 469
 Koch, D. G., et al. 2010, *ApJ*, 713, L131
 Koenigl, A. 1991, *ApJ*, 370, L39
 Kovács, G., et al. 2007, *ApJ*, 670, L41
 Kozai, Y. 1962, *AJ*, 67, 591
 Kraft, R. P. 1967, *ApJ*, 150, 551
 Latham, D. W., et al. 2009, *ApJ*, 704, 1107
 Latham, D. W., et al. 2010, *ApJ*, 713, L140
 Laughlin, G., Wolf, A., Vanmunster, T., Bodenheimer, P., Fischer, D., Marcy, G., Butler, P., & Vogt, S. 2005, *ApJ*, 621, 1072
 Léger, A., et al. 2009, *A&A*, 506, 287
 Lin, D. N. C., Bodenheimer, P., & Richardson, D. C. 1996, *Nature*, 380, 606
 Lister, T. A., et al. 2009, *ApJ*, 703, 752
 Marcy, G. W., Butler, R. P., Fischer, D. A., & Vogt, S. S. 2004, *Extrasolar Planets: Today and Tomorrow*, 321, 3
 Marigo, P., Girardi, L., Bressan, A., Groenewegen, M. A. T., Silva, L., & Granato, G. L. 2008, *A&A*, 482, 883
 Marzari, F., & Weidenschilling, S. J. 2002, *Icarus*, 156, 570
 Matt, S., & Pudritz, R. E. 2005, *ApJ*, 632, L135
 McCullough, P. R., et al. 2006, *ApJ*, 648, 1228
 McCullough, P. R., et al. 2008, *arXiv:0805.2921*
 McLaughlin, D. B. 1924, *ApJ*, 60, 22
 McNally, D. 1965, *The Observatory*, 85, 166
 Melo, C., Santos, N. C., Pont, F., Guillot, T., Israelian, G., Mayor, M., Queloz, D., & Udry, S. 2006, *A&A*, 460, 251
 Mestel, L. 1968, *MNRAS*, 138, 359
 Moutou, C., et al. 2008, *A&A*, 488, L47
 Nagasawa, M., Ida, S., & Bessho, T. 2008, *ApJ*, 678, 498
 Narita, N., et al. 2007, *PASJ*, 59, 763
 Narita, N., Sato, B., Hirano, T., & Tamura, M. 2009, *PASJ*, 61, L35
 Narita, N., Sato, B., Hirano, T., Winn, J. N., Aoki, W., & Tamura, M. 2010, *arXiv:1003.2268*
 Noyes, R. W., et al. 2008, *ApJ*, 673, L79

- Nutzman, P., Charbonneau, D., Winn, J. N., Knutson, H. A., Fortney, J. J., Holman, M. J., & Agol, E. 2009, *ApJ*, 692, 229
- Ogihara, M., & Ida, S. 2009, *ApJ*, 699, 824
- Ohta, Y., Taruya, A., & Suto, Y. 2005, *ApJ*, 622, 1118
- Pál, A., et al. 2008, *ApJ*, 680, 1450
- Pál, A., et al. 2009, *ApJ*, 700, 783
- Pál, A., et al. 2010, *MNRAS*, 401, 2665
- Papaloizou, J. C. B., & Terquem, C. 2001, *MNRAS*, 325, 221
- Pollacco, D., et al. 2008, *MNRAS*, 385, 1576
- Pont, F. 2009, *MNRAS*, 396, 1789
- Pont, F., et al. 2009, *A&A*, 502, 695
- Prosser, C. F., et al. 1995, *PASP*, 107, 211
- Radick, R. R., Thompson, D. T., Lockwood, G. W., Duncan, D. K., & Baggett, W. E. 1987, *ApJ*, 321, 459
- Rauer, H., et al. 2009, *A&A*, 506, 281
- Rossiter, R. A. 1924, *ApJ*, 60, 15
- Santos, N. C., et al. 2004, *A&A*, 426, L19
- Sato, B., et al. 2005, *ApJ*, 633, 465
- Scholz, A., & Eislöffel, J. 2007, *MNRAS*, 381, 1638
- Skillen, I., et al. 2009, *A&A*, 502, 391
- Skumanich, A. 1972, *ApJ*, 171, 565
- Shporer, A., et al. 2009, *ApJ*, 690, 1393
- Shu, F., Najita, J., Ostriker, E., Wilkin, F., Ruden, S., & Lizano, S. 1994, *ApJ*, 429, 781
- Snellen, I. A. G., et al. 2009, *A&A*, 497, 545
- Southworth, J. 2008, *MNRAS*, 386, 1644
- Southworth, J., et al. 2009, *MNRAS*, 396, 1023
- Southworth, J., et al. 2009, *ApJ*, 707, 167
- Sozzetti, A., Torres, G., Charbonneau, D., Latham, D. W., Holman, M. J., Winn, J. N., Laird, J. B., & O'Donovan, F. T. 2007, *ApJ*, 664, 1190
- Sozzetti, A., et al. 2009, *ApJ*, 691, 1145
- Tassoul, J.-L. 2000, *Stellar rotation* / Jean-Louis Tassoul. Cambridge ; New York : Cambridge University Press, 2000. (Cambridge astrophysics series ; 36),
- Terquem, C., & Papaloizou, J. C. B. 2002, *MNRAS*, 332, L39
- Terquem, C., & Papaloizou, J. C. B. 2007, *ApJ*, 654, 1110
- Thommes, E. W., & Lissauer, J. J. 2003, *ApJ*, 597, 566
- Torres, G., et al. 2007, *ApJ*, 666,
- Torres, G., Winn, J. N., & Holman, M. J. 2008, *ApJ*, 677, 1324
- Torres, G., et al. 2010, *ApJ*, 715, 458
- Triaud, A. H. M. J., et al. 2009, *A&A*, 506, 377
- Valenti, J. A., & Fischer, D. A. 2005, *ApJS*, 159, 14
- Ward, W. R. 1997, *Icarus*, 126, 261
- Weber, E. J., & Davis, L., Jr. 1967, *ApJ*, 148, 217
- West, R. G., et al. 2009, *AJ*, 137, 4834
- Winn, J. N., et al. 2005, *ApJ*, 631, 1215
- Winn, J. N., et al. 2007, *AJ*, 133, 1828
- Winn, J. N., et al. 2008, *ApJ*, 683, 1076
- Winn, J. N., et al. 2009, *ApJ*, 693, 794
- Winn, J. N., Johnson, J. A., Albrecht, S., Howard, A. W., Marcy, G. W., Crossfield, I. J., & Holman, M. J. 2009, *ApJ*, 703, L99
- Yu, Q., & Tremaine, S. 2001, *AJ*, 121, 1736

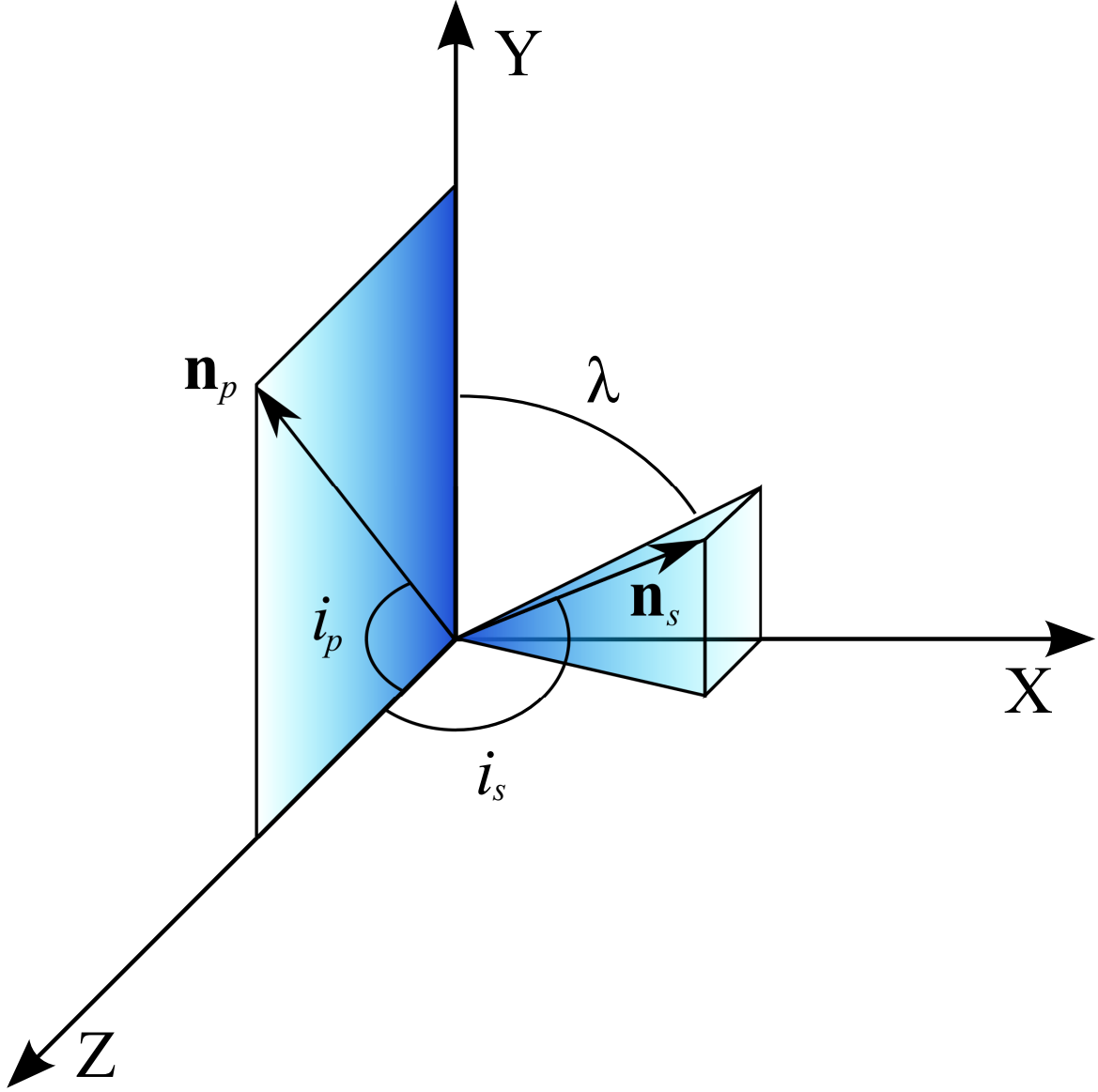


Figure 1. The geometry of transiting exoplanet systems following the conventions described in Fabrycky & Winn (2009), with the z -axis oriented toward the observer. The exoplanet orbit is defined by the vector \mathbf{n}_p and is inclined at an angle i_p to the observer's line of sight. The host stellar spin is defined by the vector \mathbf{n}_s and is inclined at an angle i_s to the observer's line of sight. Transit measurements can determine i_p , and measurements of the Rossiter-McLaughlin effect can reveal λ , the angle in the xy -plane between the projection of \mathbf{n}_p and \mathbf{n}_s (Rossiter 1924; McLaughlin 1924; Ohta et al. 2005). The angle i_s is difficult to measure for individual stars, but as I show in this paper, it may be possible to identify systems in which i_s and i_p are misaligned by a large degree.

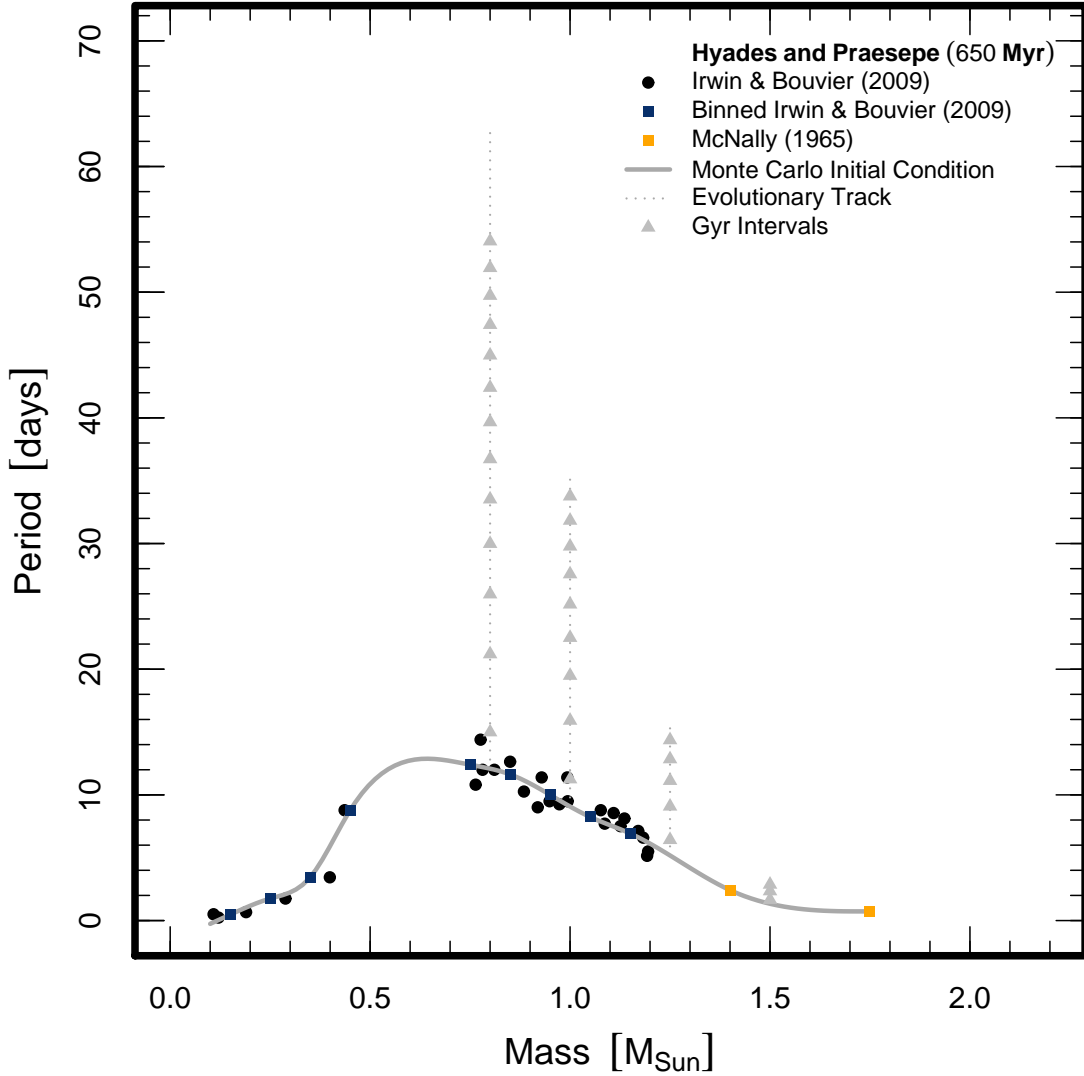


Figure 2. Stellar rotation period of Sun-like stars as a function of mass and age. Though a population of Sun-like stars is formed with a wide range of rotation periods P_* (Attridge & Herbst 1992; Choi & Herbst 1996), by the time that population is the age of the Hyades and Praesepe period is only a function of mass (e.g. Tassoul 2000; Irwin & Bouvier 2009). Main sequence stars lose angular momentum and evolve from from this initial condition, likely through a magnetized stellar wind (e.g. Weber & Davis 1967; Mestel 1968; Kawaler 1988). As a result, stellar periods increase on the main sequence as they age (e.g. Kraft 1967) as $P_* \propto t^{1/2}$, in accordance with the empirical relation $v \sin i \propto t^{-1/2}$ noted by Skumanich (1972). I binned the available Hyades and Praesepe data (Radick et al. 1987; Prosser et al. 1995; Scholz & Eislöffel 2007) as summarized in Irwin & Bouvier (2009) (black points) in bins of $0.1 M_{\odot}$ (blue squares), supplemented it with average rotation values for higher mass field stars (McNally 1965) (orange squares), and used natural cubic spline interpolation to compute a relationship between mass and period for stars between $0.2 M_{\odot} \lesssim M_* \lesssim 1.75 M_{\odot}$ (solid gray curve). From this initial condition, I evolve the rotation period as $P_* \propto t^{1/2}$ (dotted gray vertical lines). The length of the vertical lines correspond to the main sequence lifetime of a star of the given mass, and I denote Gyr intervals (from 1 Gyr to 13 Gyr) with gray triangles along each vertical line.

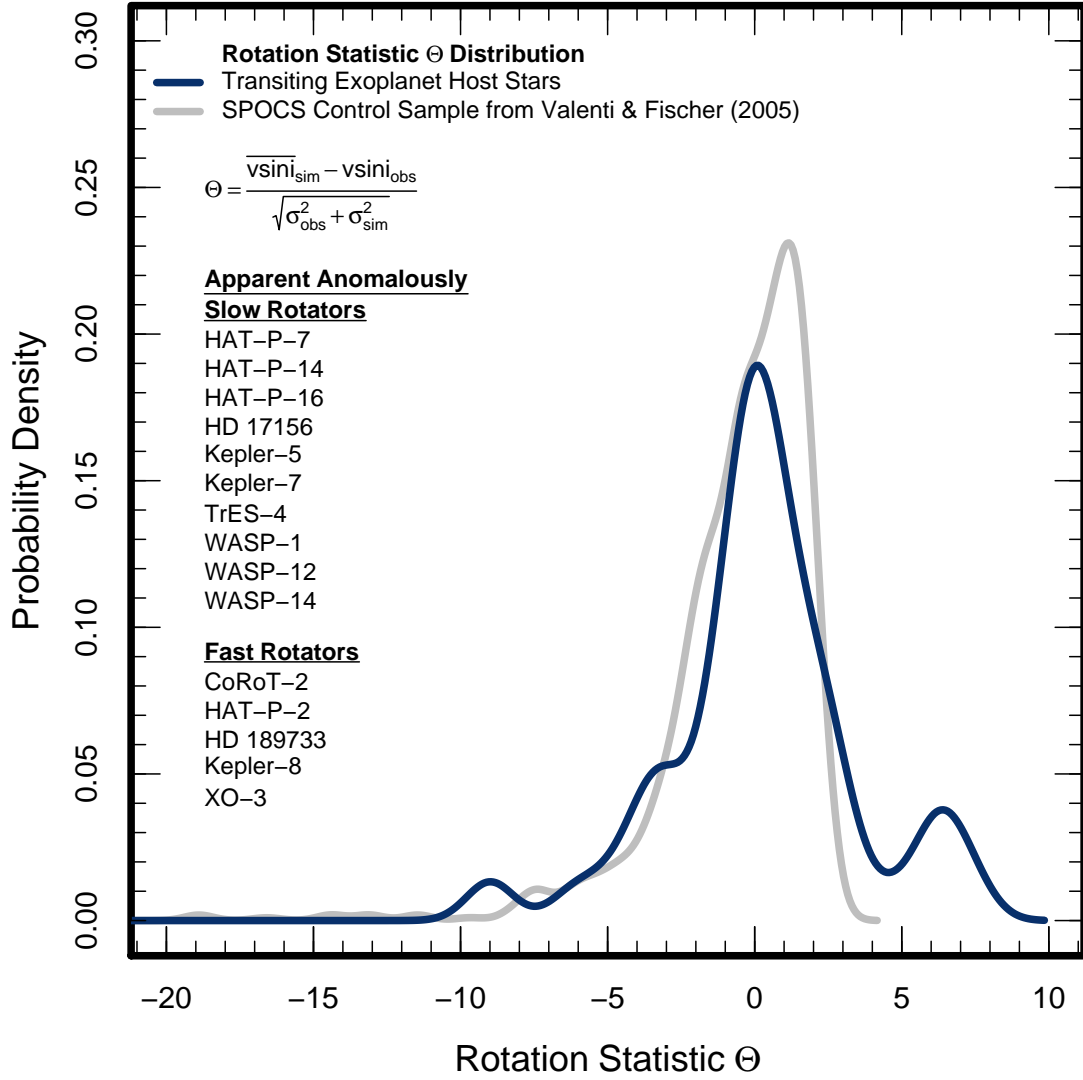


Figure 3. The distribution of the rotation statistic Θ for stars that host transiting exoplanets (solid blue line) compared to a control sample from the SPOCS catalog of Valenti & Fischer (2005) (solid gray line). I define $\Theta \equiv (\overline{v \sin i}_{\text{sim}} - v \sin i_{\text{obs}}) / \sqrt{\sigma_{\text{obs}}^2 + \sigma_{\text{sim}}^2}$ such that stars that have a $v \sin i$ smaller (larger) than expected given their mass, age, radius, and the uncertainties in those parameters have positive (negative) values of Θ . By comparison with the control sample, transiting exoplanet host stars that have $\Theta > 2.9$ have $v \sin i$ so small that they cannot be explained by evolving the Hyades and Praesepe data according to the $P_* \propto t^{1/2}$ relation given the system parameters and uncertainties and assuming alignment between the exoplanet orbit and the spin of its host. I argue that unless these stellar hosts of transiting exoplanets are slower rotators relative to the model than any of the 866 stars in the SPOCS control sample, the most natural explanation for this result is that i_s and i_p are misaligned.

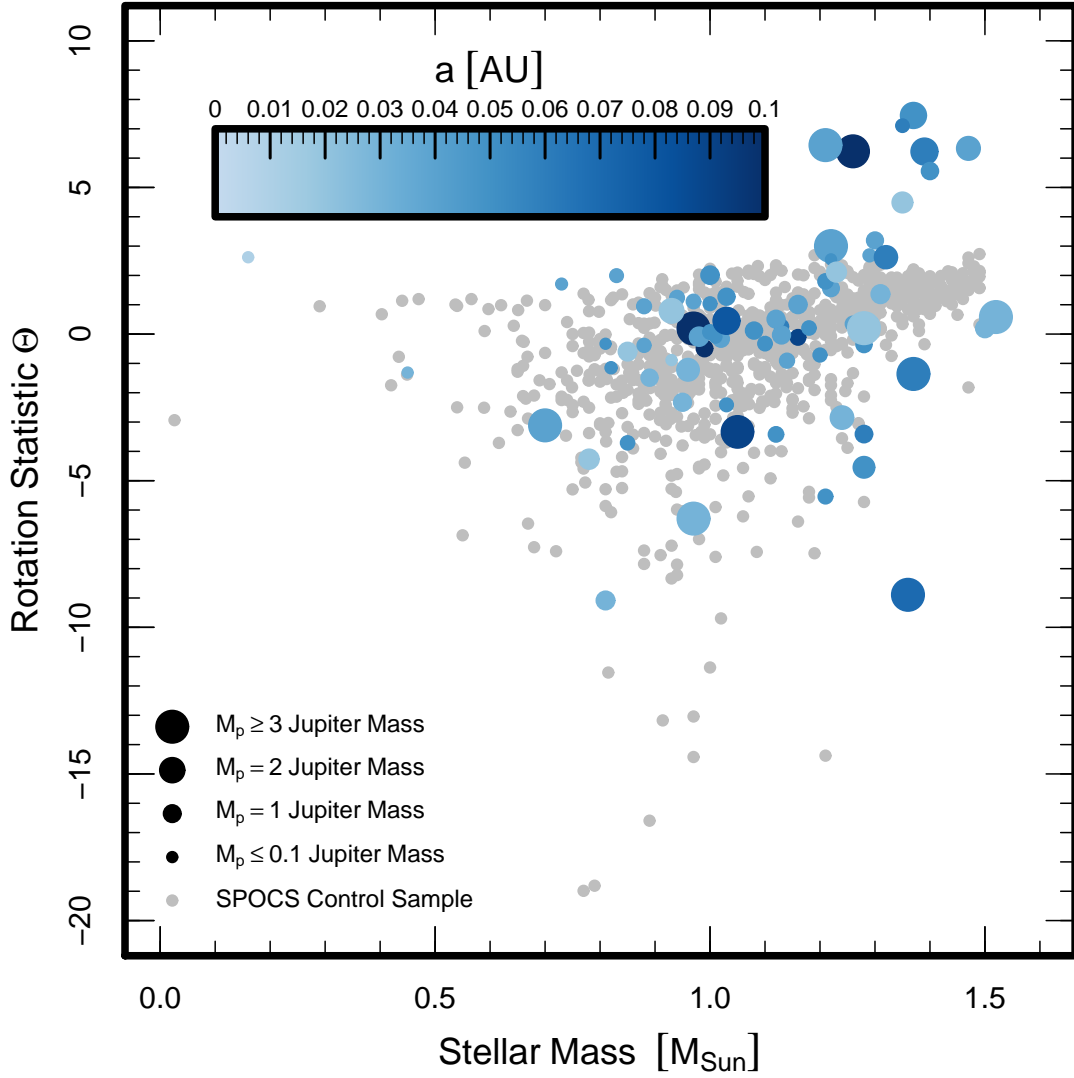


Figure 4. The rotation statistic Θ as a function of stellar mass for both stars that host transiting exoplanets (blue points) and control stars from the SPOCS catalog (gray points). Note that stars with $\Theta > 2.9$ – anomalously slow projected rotation assuming spin-orbit alignment – are preferentially massive. In the sample of 75 systems in Table 1, the probability that all ten misaligned systems have host stellar mass in the range $1.2 M_{\odot} \lesssim M_{\star} \lesssim 1.5 M_{\odot}$ by chance is less than one in ten thousand. In addition, the exoplanet host stars with $\Theta > 2.9$ host planets with a range of semimajor axes, not just those at small semimajor axes where tidal forces are most important. In any case, the rotation period of each exoplanet host star with $\Theta > 2.9$ is expected to be longer than the orbital period of its planet, so those stars are unlikely to transfer angular momentum to their planets.

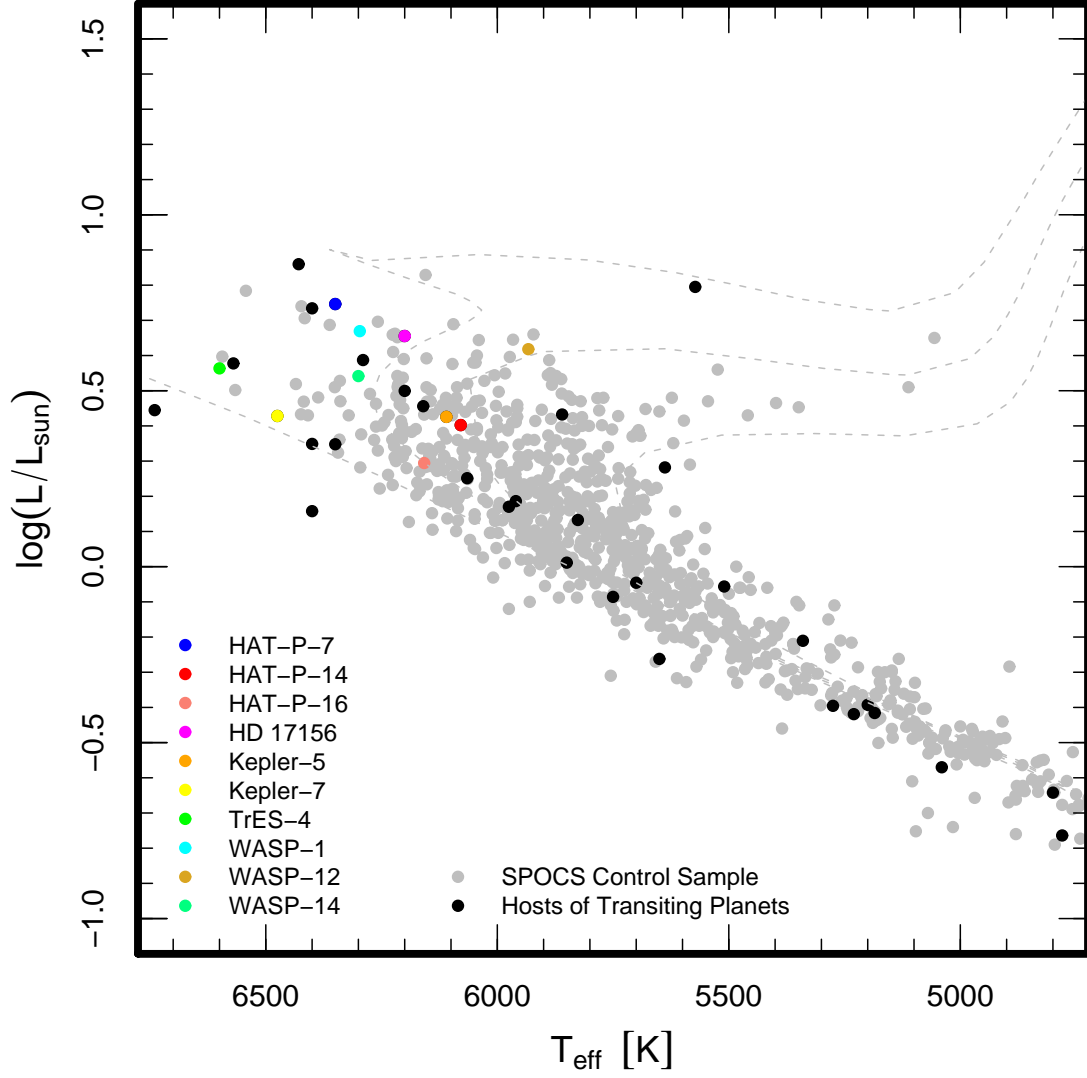


Figure 5. A theoretical HR diagram of the control sample of SPOCS stars (gray points) overplotted with the anomalously slow projected rotators identified in this analysis. I also plot other hosts of transiting exoplanets with precise trigonometric parallaxes (black points). The dashed lines are Padova isochrones for ages 0.1, 3, 5, and 10 Gyr (Marigo et al. 2008). There are both young and evolved stars in the control sample, so the SPOCS sample is a fair control sample in regards to evolutionary state. In addition, the fact that there are evolved hosts of transiting exoplanets that are not identified as anomalously slow projected rotators suggests that the rotational evolution of evolved main sequence stars alone cannot explain the anomalously slow projected rotation identified in some systems.

Table 1
Transiting Exoplanet System Properties

System	M_* [M_\odot]	R_* [R_\odot]	τ_L [Gyr]	τ_U [Gyr]	$v \sin i_{obs}$ [km s $^{-1}$]	σ_{obs} [km s $^{-1}$]	i_p [deg]	$\overline{v \sin i_{sim}}$ [km s $^{-1}$]	σ_{sim} [km s $^{-1}$]	Θ	Reference
CoRoT-1	0.95	1.11	5.20	1.00	85.10	2.17	0.87	-2.28	1
CoRoT-2	0.97	0.90	0.20	4.00	11.85	0.50	87.84	3.10	1.27	-6.43	2,3
CoRoT-3	1.37	1.56	1.60	2.80	17.00	1.00	85.90	14.92	1.21	-1.32	4
CoRoT-4	1.16	1.17	0.70	2.00	6.40	1.00	90.00	6.23	0.93	-0.12	5,6
CoRoT-5	1.00	1.19	5.50	8.30	1.00	1.00	85.83	2.05	0.12	1.04	7
CoRoT-6	1.05	1.03	1.00	3.30	7.50	1.00	89.07	3.62	0.62	-3.29	8
CoRoT-7	0.93	0.87	1.20	2.30	3.50	...	80.10	2.57	0.24	-0.91	9
CoRoT-9	0.99	0.94	0.15	8.00	3.50	...	89.99	2.66	1.54	-0.46	10
GJ 436	0.45	0.46	1.00	10.00	2.40	...	85.80	1.03	0.35	-1.30	11,12,13
GJ 1214	0.16	0.21	3.00	10.00	2.00	...	88.62	5.65	0.96	2.63	14
HAT-P-1	1.13	1.12	0.70	5.20	3.75	0.58	86.28	4.06	1.16	0.24	12,15
HAT-P-2	1.36	1.64	2.10	3.10	20.80	0.30	86.72	13.60	0.77	-8.72	16
HAT-P-3	0.94	0.82	0.10	6.90	0.50	0.50	87.24	2.19	1.24	1.26	17
HAT-P-4	1.26	1.59	3.60	6.80	5.50	0.50	89.90	5.81	0.53	0.42	18
HAT-P-5	1.16	1.17	1.20	4.70	2.60	1.50	86.75	4.31	0.82	1.00	12,19
HAT-P-6	1.29	1.46	1.70	2.80	8.70	1.00	85.51	9.09	0.66	0.33	12,20
HAT-P-7	1.47	1.84	1.20	3.20	3.80	0.50	85.70	32.66	4.61	6.23	21
HAT-P-8	1.28	1.58	2.40	4.40	11.50	0.50	87.50	7.77	0.67	-4.45	22
HAT-P-9	1.28	1.32	0.20	3.40	11.90	1.00	86.50	9.95	3.87	-0.49	23
HAT-P-11	0.81	0.75	2.40	12.40	1.50	1.50	88.50	1.00	0.24	-0.33	24
HAT-P-12	0.73	0.70	0.50	4.50	0.50	0.40	89.00	1.62	0.52	1.72	25
HAT-P-13	1.22	1.56	4.30	7.50	2.90	1.00	83.40	4.54	0.36	1.54	26
HAT-P-14	1.39	1.47	0.90	1.70	8.40	0.50	83.50	20.57	1.91	6.16	27
HAT-P-16	1.22	1.24	1.20	2.80	3.50	0.50	86.60	6.32	0.78	3.03	28
HD 17156	1.26	1.45	2.30	3.70	2.60	0.50	86.20	6.86	0.48	6.15	29,30
HD 80606	0.97	0.98	1.80	1.00	89.29	2.08	0.85	0.21	31,32,33
HD 149026	1.29	1.50	1.00	2.80	6.00	0.50	85.40	10.32	1.51	2.71	12,34,35
HD 189733	0.81	0.76	2.40	12.00	3.32	0.05	85.76	1.03	0.23	-9.75	12,36,37
HD 209458	1.12	1.16	2.40	3.90	4.70	0.16	86.55	3.66	0.26	-3.45	12,38
Kepler-4	1.22	1.49	3.00	6.00	2.20	1.00	89.76	5.04	0.49	2.55	39
Kepler-5	1.37	1.79	2.40	3.60	4.80	1.00	86.30	14.63	0.87	7.41	40
Kepler-6	1.21	1.39	2.80	4.80	3.00	1.00	86.80	4.95	0.38	1.82	41
Kepler-7	1.35	1.84	2.50	4.50	4.20	0.50	86.50	12.51	1.05	7.13	42
Kepler-8	1.21	1.49	2.34	5.34	10.50	0.70	84.07	5.30	0.64	-5.48	43
OGLE-TR-10	1.14	1.17	0.10	7.20	7.00	1.00	83.87	4.52	2.70	-0.86	12,44,45
OGLE-TR-56	1.23	1.36	1.90	4.20	3.20	1.00	79.80	5.72	0.65	2.12	12,44,45
OGLE-TR-111	0.85	0.83	2.20	14.00	5.00	...	88.10	1.11	0.29	-3.73	12,44,45
OGLE-TR-113	0.78	0.77	10.80	14.00	5.00	...	89.40	0.73	0.03	-4.27	12,44,46
OGLE-TR-132	1.31	1.32	0.10	2.70	5.00	...	83.30	14.01	6.69	1.33	12,44,45
OGLE2-TR-L9	1.52	1.53	0.00	0.66	39.33	0.38	79.80	128.20	205.72	0.43	47
TrES-1	0.88	0.81	0.90	7.10	1.08	0.30	88.40	1.64	0.47	0.99	12,48,49
TrES-2	0.98	1.00	2.90	7.70	2.00	1.00	83.62	1.92	0.27	-0.08	12,50,51
TrES-3	0.93	0.83	0.10	3.70	1.50	1.00	81.85	2.88	1.53	0.76	52
TrES-4	1.40	1.81	2.50	4.40	8.50	0.50	82.86	16.49	1.34	5.60	51,52
WASP-1	1.30	1.52	2.40	3.60	5.00	...	88.25	8.58	0.50	3.20	12,45,53
WASP-2	0.89	0.84	0.00	14.00	5.00	...	84.80	1.61	1.72	-1.71	12,51,53
WASP-3	1.24	1.31	0.70	3.50	13.40	1.50	85.06	7.37	1.70	-2.66	54,55
WASP-4	0.85	0.87	2.00	9.00	2.00	1.00	89.35	1.37	0.29	-0.61	56
WASP-5	0.96	1.03	1.10	9.80	3.50	1.00	85.80	2.02	0.63	-1.25	56,57
WASP-6	0.88	0.87	4.00	18.00	1.40	1.00	88.47	1.02	0.22	-0.37	58
WASP-7	1.28	1.24	17.00	2.00	89.60	6.98	2.13	-3.43	59
WASP-8	1.03	0.95	3.00	5.00	2.00	0.60	88.52	2.29	0.17	0.46	60
WASP-10	0.70	0.78	0.60	1.00	6.00	...	86.90	2.82	0.20	-3.12	61
WASP-11/HAT-P-10	0.83	0.79	4.10	11.70	0.50	0.20	88.60	0.99	0.15	1.96	62
WASP-12	1.35	1.57	1.00	3.00	2.20	1.50	83.10	14.26	2.19	4.55	63
WASP-13	1.03	1.34	3.60	14.00	4.90	...	86.90	2.25	0.44	-2.43	64
WASP-14	1.21	1.31	0.50	1.00	2.80	0.57	84.32	10.45	1.05	6.39	65,66
WASP-15	1.18	1.48	2.60	6.70	4.00	2.00	85.50	4.40	0.57	0.19	67
WASP-16	1.02	0.95	0.10	8.10	3.00	1.00	85.22	2.71	1.63	-0.15	68
WASP-17	1.20	1.38	0.40	3.90	9.00	1.50	87.80	6.95	2.25	-0.76	69
WASP-18	1.28	1.23	0.00	2.00	11.00	1.50	86.00	15.25	14.39	0.29	70,71
WASP-19	0.96	0.94	1.00	14.50	4.00	2.00	80.50	1.58	0.59	-1.16	72
WASP-21	1.01	1.06	7.00	17.00	1.50	0.60	88.75	1.43	0.18	-0.11	73
WASP-22	1.10	1.13	1.00	...	3.50	0.60	89.20	3.21	0.95	-0.26	74
WASP-24	1.13	1.15	0.00	3.70	6.96	...	85.71	7.46	11.68	0.04	75
WASP-25	1.00	0.95	0.40	4.60	3.00	1.00	87.70	3.06	1.06	0.04	76
WASP-26	1.12	1.34	4.00	8.00	2.40	1.30	82.50	3.06	0.31	0.49	77
WASP-28	1.08	1.05	3.00	8.00	2.20	1.60	89.10	2.39	0.33	0.11	78
WASP-29	0.82	0.85	10.00	...	1.50	0.60	87.96	0.80	0.06	-1.15	79
WASP-33	1.50	1.44	0.00	0.50	90.00	10.00	87.67	131.62	200.45	0.21	80
XO-1	1.03	0.93	0.10	4.10	1.11	0.67	89.06	3.76	1.96	1.28	12,45,81
XO-2	0.97	0.98	3.90	8.70	1.30	0.30	88.90	1.69	0.20	1.08	82,83
XO-3	1.21	1.38	2.00	3.40	18.54	0.17	84.20	5.79	0.44	-27.04	84,85
XO-4	1.32	1.56	1.50	2.70	8.80	0.50	88.70	11.76	1.02	2.61	86

Table 1 — *Continued*

System	M_* [M_\odot]	R_* [R_\odot]	τ_L [Gyr]	τ_U [Gyr]	$v \sin i_{obs}$ [km s $^{-1}$]	σ_{obs} [km s $^{-1}$]	i_p [deg]	$\overline{v \sin i_{sim}}$ [km s $^{-1}$]	σ_{sim} [km s $^{-1}$]	Θ	Reference
XO-5	1.00	1.11	7.70	9.30	0.70	0.50	86.80	1.71	0.05	2.01	87,88

Note. — (1) Barge et al. (2008); (2) Alonso et al. (2008); (3) Bouchy et al. (2008); (4) Deleuil et al. (2008); (5) Aigrain et al. (2008); (6) Moutou et al. (2008); (7) Rauer et al. (2009); (8) Fridlund et al. (2010); (9) Léger et al. (2009); (10) Deeg et al. (2010); (11) Santos et al. (2004); (12) Torres et al. (2008); (13) Bean et al. (2008); (14) Charbonneau et al. (2009); (15) Johnson et al. (2008); (16) Pál et al. (2010); (17) Torres et al. (2007); (18) Kovács et al. (2007); (19) Bakos et al. (2007b); (20) Noyes et al. (2008); (21) Pál et al. (2008); (22) Latham et al. (2009); (23) Shporer et al. (2009); (24) Bakos et al. (2010); (25) Hartman et al. (2009); (26) Bakos et al. (2009b); (27) Torres et al. (2010); (28) Buchhave et al. (2010); (29) Fischer et al. (2007); (30) Winn et al. (2009a); (31) Fischer & Valenti (2005); (32) Pont et al. (2009); (33) Fossey et al. (2009); (34) Sato et al. (2005); (35) Nutzman et al. (2009); (36) Winn et al. (2007); (37) Triaud et al. (2009); (38) Winn et al. (2005); (39) Borucki et al. (2010); (40) Koch et al. (2010); (41) Dunham et al. (2010); (42) Latham et al. (2010); (43) Jenkins et al. (2010); (44) Melo et al. (2006); (45) Southworth (2008); (46) Gillon et al. (2006); (46) Snellen et al. (2009); (48) Laughlin et al. (2005); (49) Narita et al. (2007); (47) Sozzetti et al. (2007); (51) Daemgen et al. (2009); (52) Sozzetti et al. (2009); (53) Cameron et al. (2007); (54) Pollacco et al. (2008); (55) Gibson et al. (2008); (56) Gillon et al. (2009a); (57) Southworth et al. (2009a); (58) Gillon et al. (2009b); (59) Hellier et al. (2009a); (60) Queloz et al. (2010, submitted); (61) Christian et al. (2009); (62) Bakos et al. (2009a); (63) Hebb et al. (2009); (64) Skillen et al. (2009); (65) Joshi et al. (2009); (66) Johnson et al. (2009); (67) West et al. (2009); (68) Lister et al. (2009); (69) Anderson et al. (2010); (70) Hellier et al. (2009b); (71) Southworth et al. (2009b); (72) Hebb et al. (2010); (73) Bouchy et al. (2010, submitted); (74) Maxted et al. (2010, submitted); (75) Street et al. (2010, submitted); (76) Enoch et al. (2010, submitted); (77) Smalley et al. (2010, submitted); (78) West et al. (2010, submitted); (79) Hellier et al. (2010, submitted); (80) Cameron et al. (2010, submitted); (81) McCullough et al. (2006); (82) Burke et al. (2007); (83) Fernandez et al. (2009); (84) Johns-Krull et al. (2008); (85) Winn et al. (2008); (86) McCullough et al. (2008); (87) Burke et al. (2008); (88) Pál et al. (2009b)

Table 2
Misalignment Properties

System	i_p [deg]	$i_{s,1}$ [deg]	$i_{s,2}$ [deg]	$i_{s,3}$ [deg]	$i_{s,4}$ [deg]	λ [deg]	Reference
HAT-P-7 b	85.70	6.7	170	190	350	-177.5	Winn et al. (2009b)
HAT-P-14 b	83.50	24	160	200	340	...	
HAT-P-16 b	86.60	34	150	210	330	...	
HD 17156 b	86.20	22	160	200	340	10	Narita et al. (2009)
Kepler-5 b	86.30	19	160	200	340	...	
Kepler-7 b	86.50	20	160	200	340	...	
TrES-4	82.86	31	150	210	330	-6.3	Narita et al. (2010)
WASP-1 b	88.25	36	140	220	320	...	
WASP-12 b	83.10	8.8	170	190	350	...	
WASP-14 b	84.32	15	160	200	340	-33.1	Johnson et al. (2009)

Note. — Column 2 is the inclination of the transiting planet’s orbit to the line of sight i_p . Columns 3 through 6 are the four possible values of i_s given the value of $\sin i$ inferred from the difference in $v \sin i_{obs}$ and $v \sin i_{sim}$. Column 7 is the measured value of λ from the Rossiter-McLaughlin measurement taken from the indicated reference.